2024 IEEE International Conference on Robotics and Automation (ICRA 2024)
May 13-17, 2024. Yokohama, Japan

Learning Contact for Haptic Feedback: Switching X-lateral Teleoperators

Nural Yilmaz[1,2], Ugur Tumerdem[1,3]

Abstract— **In this paper, we propose X-lateral teleoperation: a novel hybrid unilateral-bilateral teleoperation framework. Bilateral teleoperation enables kinesthetic coupling between the operator and the remote environment with haptic feedback. However, in free motion, unlike unilateral teleoperators, bilateral teleoperators reflect undesirable operational forces to the operator. The proposed X-lateral teleoperation framework benefits from a learning-based contact detection algorithm which triggers switching from unilateral teleoperation in free motion to bilateral teleoperation in contact. We also present a neural network based two-class classification technique to detect contacts even with environments not seen in training. In experiments with linear motors and Phantom Omni devices, using sensorless force estimation, we show that the proposed method can decrease operational forces significantly over transparency-optimized bilateral architectures.**

I. INTRODUCTION

In bilateral teleoperation, information transfer between the local and remote systems is two-directional and measured positions and/or forces from the remote manipulator are reflected to the operator through a robotic/haptic manipulandum. While in theory it is possible to achieve ideal kinesthetic coupling/transparency between the operator and remote environment using transparency-optimized bilateral control laws [1]–[3], in practice fundamental limitations in control such as computation/communication delays, sensing/measurement noise, estimation errors or modeling uncertainty undermine transparency. An important issue is operationality [4], which causes phantom forces to be felt by the operator in addition to the environment force, even in free motion. On the other hand, in unilateral teleoperation, impedance-type master devices are typically passive, intrinsically stable and only the inertia is felt in free motion.

The main contribution of this work is in combining the advantages of unilateral and bilateral teleoperation by means of a switching control law to improve overall system transparency. In the proposed framework, unilateral control is employed when the remote manipulator is in free motion and transparency-optimized bilateral control is utilized when the remote robot contacts the environment. Thus, it is possible to eliminate the operationality of the bilateral control system in free motion and provide kinesthetic coupling/haptic feedback in contact. This approach significantly improves transparency in free motion while keeping the system stable.

Another contribution of this work is a generalizable learning-based contact detection algorithm (CDA) which can be used to detect contact with a wide range of environments, even without being specifically trained for them. To improve transparency, this algorithm can be employed as an event trigger in the switching teleoperator architecture that is proposed in this work, which will be termed X-lateral due to the transition between unilateral and bilateral controllers.

[1]Dept. of Mechanical Engineering, Marmara University, Istanbul, Turkey
[2]Dept. of Computer Science, [3]Dept. of Mechanical Engineering, Johns Hopkins University, Baltimore, MD 21218, USA (email: {nyilmaz2@jhu.edu, ugur@jhu.edu)

II. RELATED WORK

A. Bilateral Teleoperation and Transparency

Various control architectures have been proposed in the literature to achieve transparency in bilateral teleoperation. In [1], it was shown that ideal transparency can be quantified by a frequency-dependent hybrid matrix relating master and remote robot velocities and forces. In [2], [3], it was shown that classical two-channel architectures with position or force information exchange between the robots cannot satisfy transparency conditions and that four channels for the exchange of both position and force information is necessary for ideal transparency. In [4], reproducibility and operationality concepts were introduced. Reproducibility quantifies the reproduction of the environmental impedance on the operator interface and operationality quantifies the added control system impedance. In practice, zero operationality cannot be achieved due to factors like model uncertainty and latency. Improved transparency under communication delays can be achieved by switching between two channel position forward, force feedback (FP) and force forward, position feedback (PF) architectures [5]. Controller switching was also adopted in other works to improve performance. In [6], a multi-model predictive controller with different switching modes for free motion, soft contact and contact with rigid environments was proposed. In [7]–[9], gain and controller switching based on environment stiffness was proposed. However, our approach to make the master robot passive in free motion and fully actuated in contact, has not been considered before. Researchers have proposed passive master devices with brakes instead of actuators [10], which can apply resistance on the operator hand to modulate forces during contact with the environment [11]. However, estimation and control of forces on such devices is an open research problem [12], which makes it very difficult to implement transparency-optimized control.

B. Contact Detection in Robotics

Collision/contact detection has been studied extensively in robotics for safety. It is possible to use tactile sensors [13]–[16] or actuator currents/torques [17]–[19] for contact/collision detection. In [20], disturbance estimates, and in

[21], total energy and momentum was used to detect collision on robot manipulators. Threshold methods can be useful in detecting collisions with significantly higher joint torques [22], [23], but may not perform as well with softer contacts.

Recently, researchers have been using machine learning and neural network classifiers [24] for robotic contact/collision detection. In [25], one-dimensional convolutional networks (CNN), in [26] support vector machines (SVM) and CNN were used to detect collisions. While these systems can have good performance, they need training with all possible types of contact data. To overcome this issue, in [27], two unsupervised anomaly detection methods (SVM and autoencoders) were proposed. In [28], one class SVM-based collision detection and in [29] a sliding-window convolutional variational autoencoder-based collision detection was investigated. While much work has been done on the detection of collisions, which take place in milliseconds [27], detection of contacts for extended periods with various environments ranging from extremely soft to extremely hard, as is typical in haptic interaction, is still an open problem.

III. Method

A. Bilateral Teleoperation and Transparency

In a single degree of freedom linear bilateral teleoperation system ideal transparency or kinesthetic coupling requires position and velocity tracking as well as force reflection:

$$x_m = x_r \tag{1}$$
$$v_m = v_r \tag{2}$$
$$F_m = -F_r \tag{3}$$

where x, v and F respectively denote positions, velocities and external forces and the subscripts m and r denote the master and remote robot. The hybrid matrix, $\mathcal{H}$ [1], [4], is used to determine to what extent a control system is able to achieve (2)-(3):

$$\begin{bmatrix} F_m \\ v_r \end{bmatrix} = \underbrace{\begin{bmatrix} h_{11} & h_{12} \\ h_{21} & h_{22} \end{bmatrix}}_{\mathcal{H}} \begin{bmatrix} v_m \\ -F_r \end{bmatrix} \tag{4}$$

The ideal transparency conditions are obtained when:

$$h_{11} = 0, h_{12} = 1 \tag{5}$$
$$h_{21} = 1, h_{22} = 0 \tag{6}$$

The environmental impedance transmitted by the control system to the operator, Z_t, can be calculated as:

$$Z_t(s) = \frac{F_m}{v_m} = \underbrace{\frac{h_{12}}{h_{21} - h_{22}Z_e}}_{P_r} Z_e + \underbrace{\frac{h_{11}}{h_{21} - h_{22}Z_e}}_{P_o} \tag{7}$$

where P_r is the reproducibility and P_o is the operationality. For ideal transparency and environmental impedance matching: $Z_t = Z_e$, it is required that $P_r = 1$ and $P_o = 0$.

The general version of the Lawrence teleoperation architecture [2] consists of four communication channels (C_i, $i = 1:4$) between master and remote robots. C_1 and C_2 are for exchanging position measurements while C_3 and C_4 are for exchanging external force measurements. Also, the architecture includes local position controllers (C_m and C_r) and force compensators (C_5 and C_6). The linearized dynamic model of each robot can be written in frequency domain:

$$Z_m(s)v_m(s) = F_m + F_{cm} + \hat{F}_m^{dis} \tag{8}$$
$$Z_r(s)v_r(s) = F_r + F_{cr} + \hat{F}_r^{dis} \tag{9}$$

where Z_m, Z_r are the master and remote robot impedances, F_{cm}, F_{cr} are the controller outputs and $\hat{F}^{dis}$ are the optional disturbance compensation terms. The four-channel controller with force estimation can be written as:

$$F_{cm} = C_1 x_r - C_m x_m - C_5 F_m^{ext} - C_3 \hat{F}_r^{ext} \tag{10}$$
$$F_{cr} = C_2 x_m - C_r x_r - C_4 F_m^{ext} - C_6 \hat{F}_r^{ext} \tag{11}$$

where $\hat{F}_r^{ext} \approx F_r, \hat{F}_m^{ext} \approx -F_m$ are estimated external forces. When disturbance observers are used [4], four channel parameters can be selected as:

$$C_1 = C_2 = C_m = C_s = C_p = K_p + K_d s \tag{12}$$
$$C_3 = C_4 = C_5 = C_6 = C_f \tag{13}$$

Here, C_p is a PD position controller with proportional gain K_p, derivative gain K_d, and C_f is a force controller gain. This control architecture results in a hybrid matrix with:

$$h_{11} = \frac{(Z_m s + C_p)(Z_r s + C_p) - C_p^2}{C_f(Z_r s + 2C_p)} \tag{14}$$
$$h_{12} = 1, h_{21} = 1, h_{22} = 0 \tag{15}$$

Operationality and reproducibility of the teleoperation system with this controller becomes $P_r = 1$ and $P_o = h_{11}$. It can be seen that the controller can achieve ideal reproducibility but operationality is equal to the h_{11} term which is a function of the robot inertias and controller gains. If the robots can be modeled with identical pure masses M: $Z_m = Z_r = Ms$, then $P_o = h_{11} = \frac{Ms}{C_f}$. This means that an operational force of $F_m = \frac{Msv_m}{C_f}$ needs to be applied by the operator to move the master robot. If $C_f = 1$, this corresponds to the robot inertial force. While this force can be decreased by increasing C_f, it can be destabilizing [4]. Furthermore, digital controllers and communications introduce latency and the hybrid parameters are affected by time delays. Figure 1 shows how the four-channel hybrid

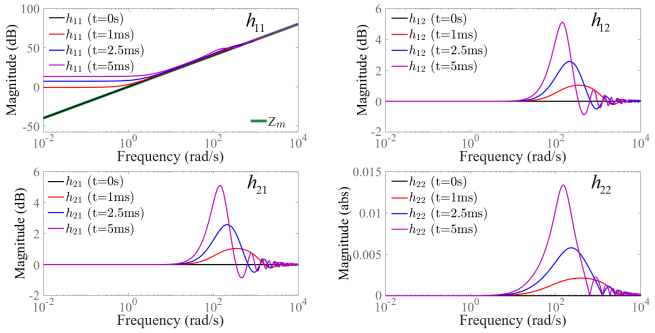

Fig. 1. The effect of time delay on hybrid matrix elements

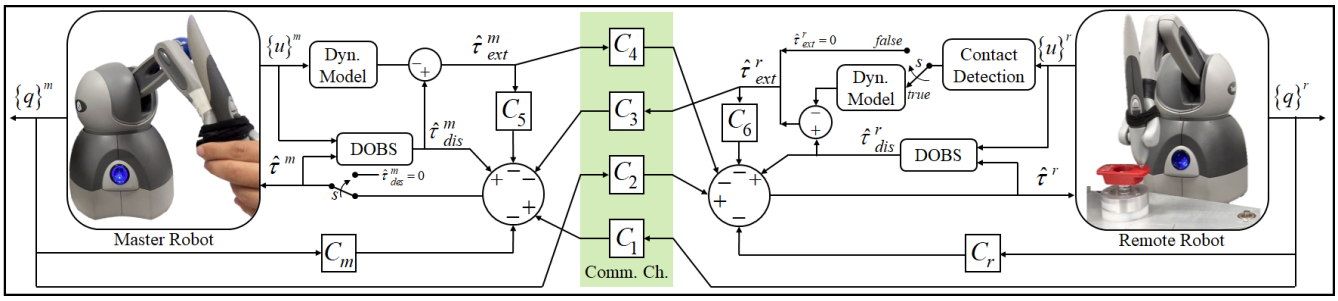

Fig. 2. Switching X-lateral teleoperation framework with disturbance observers and force estimation

parameter frequency responses are affected from time delays as small as 1 ms, which is the controller sampling time for the digital controllers in this paper. The h_{11} gain has an increase of up to 50dB at low frequencies due to time delay, which results in a heavier system than the pure inertia of the robot suggested by theory.

B. Disturbance Observers and Sensorless Force Estimation

In this work, we aim to develop a sensorless teleoperation algorithm that can also be used in robotic surgery [30]. Sensorless methods require force estimation instead of force sensing and estimation errors also increase operationality.

The nonlinear dynamic model of a robot manipulator is given with the following equation in joint space:

$$M(q)\ddot{q} + C(q,\dot{q}) + G(q) + F(\dot{q}) + \tau_{ext} = \tau \tag{16}$$

where q, $\dot{q}$ and $\ddot{q}$ denote the joint position, velocity and acceleration vectors, M, C and G represent mass/inertia matrix, Coriolis and centrifugal force/torque and gravity vectors, F refers to friction force/torque vector, τ_{ext} is the external force acting on the robot joints and τ is the joint actuation torque.

If a nominal model M_n of the actuator inertias are available this equation can be written as:

$$M_n\ddot{q} + \underbrace{\tau_{int} + \tau_{ext}}_{\tau_{dis}} = \tau \tag{17}$$

where τ_{dis} is the total disturbance and τ_{int} is the sum of internal robot forces/torques: $\tau_{int} = (M(q) - M_n)\ddot{q} + C(q,\dot{q}) + G(q) + F(\dot{q})$. The disturbance on the joints can be estimated from joint torque inputs and velocity outputs, using disturbance observers:

$$\hat{\tau}_{dis} = \frac{g_{dis}}{s + g_{dis}}(\tau + g_{dis}M_n\dot{q}) - g_{dis}M_n\dot{q} \tag{18}$$

where g_{dis} is the low-pass cut-off frequency of the disturbance observer. If the disturbance estimate is fed back to the control system, it compensates the effects of τ_{dis} within the observer bandwidth.

If an inverse dynamic model $\hat{\tau}_{dyn} \approx \tau_{int}$ is readily available or can be learned it is possible to estimate the external torques acting on the joints as [31]:

$$\hat{\tau}_{ext} = \hat{\tau}_{dis} - \hat{\tau}_{dyn} \tag{19}$$

The external force acting on the robot in the Cartesian space can then be calculated as:

$$\hat{F}_{ext} = J^{-T}\hat{\tau}_{ext} \tag{20}$$

However, it is almost impossible to obtain an exact dynamic model due to dynamic uncertainties, therefore estimation errors will also show up as operational forces:

$$F_{err} = J^{-T}\tau_{err} \tag{21}$$

where $\tau_{err} = \hat{\tau}_{ext} - \tau_{ext}$.

C. Contact Detection Algorithm

To implement a switching control law, we first propose a learning-based binary classification method to classify the robot behavior as "*contact*" or "*non-contact*" during teleoperation. The features that help in distinguishing the classes are velocity, error between master and remote robot positions, and disturbance force/torque estimates:

$$u = \begin{bmatrix}\dot{q} & q_m - q_r & \hat{\tau}_{dis}\end{bmatrix}_{1:n} \tag{22}$$

With a single degree of freedom (DOF) bilateral teleoperation system (n=1) there are 3 features in total. With Phantom Omni robots, there are 3 active joints (n=3) and 9 features as inputs to the network. Joint position vector was not included in training features since it was desired for the network to be position-independent while detecting contacts. Following hyper-parameter tuning to optimize detection accuracy and training time, a neural network was utilized with only the input layer changing between different robots with:

- 1 input layer for $3n$ input features (n: # of joints)
- 3 hidden layers, each with 40 hidden neurons
- 3 *tansig* transfer functions for the hidden layers and 1 *softmax* transfer function for the output layer
- 1 output layer for binary classification ("*contact*" or "*non-contact*")

For contact detection, {*true*,*false*} is the binary output of the network indicating contact status. During training, specified features are recorded while an operator bilaterally teleoperates the remote robot. Initially, the robot was moved in free-space without contact, collecting *non-contact* class features. Then, *contact* class features were collected when the robot contacted the environment and moved while in contact. To improve generalizability we provided training with two

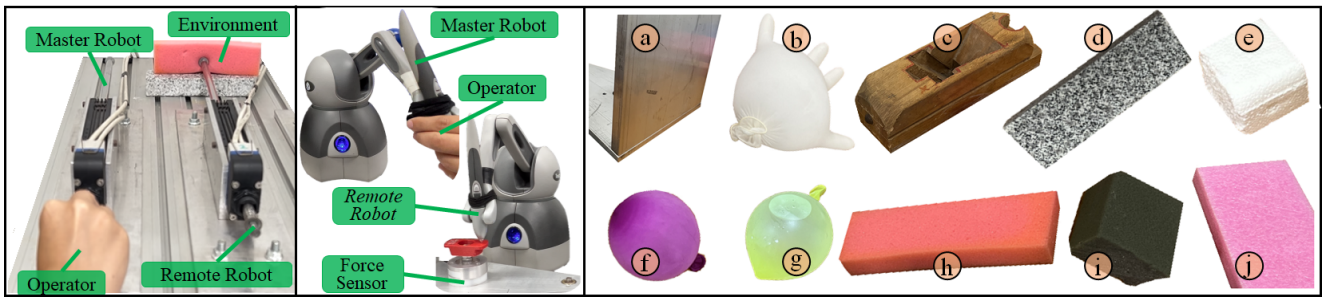

Fig. 3. Left: Robots used in the experiments Right: Objects with different stiffness values used in the experiments (a) Metal (b) Balloon 1 (c) Wood (d) Granite (e) EPS foam (f) Balloon 2 (g) Balloon with water (h) Polyurethane foam 1 (i) Polyurethane foam 2 (j) Polyethylene foam

extreme stiffness environments: balloon filled with air, and metal, and also excluded position from training features.

In Matlab, *Deep Learning Toolbox* and *Patternnet* were used to implement a pattern recognition neural network for classification. This process involved collecting a total of 435k samples at 1kHz, comprising both *non-contact* and *contact* data, with 358k samples representing the *non-contact* class ($k = 1000$ samples). The dataset was randomly split with a 70:15:15 ratio for training, validation and testing. The *mapminmax* function was employed to normalize input matrix row minimum and maximum values to [-1,1], and *cross-entropy* was used as the performance metric.

D. Switching X-lateral Teleoperation

Based on the output of the contact detection network, the teleoperation system transitions between unilateral and bilateral modes. A general block diagram for the proposed framework implemented with identical master and remote robots is presented in Fig. 2. The block diagram shows the controller implemented for each DOF of the robots as teleoperation is realized in joint space. Thus, the Phantom Omni robots in Fig. 2 can be replaced with 1-DOF motors without loss of generality. The proposed control system utilizes disturbance observers and the dynamic model $\hat{\tau}_{dyn}$ for each robot is learned with a neural network that has a Bayesian optimization function, a set of $2n$ input neurons, for position and velocity inputs, one hidden layer consisting of 20 neurons and an output layer of n neurons. The network is trained with $\hat{\tau}_{dis} \approx \tau_{int}$ (in free motion) and predicts $\hat{\tau}_{dyn}$ to obtain τ_{ext} (19). The hybrid control algorithm for each DOF can then be written as in Algorithm 1.

Algorithm 1 Switching X-Lateral Control

if $Contact = true$ **then**
$\tau_m = \hat{\tau}_m^{dis} + C_1 q_r - C_m q_m - C_5 \hat{\tau}_m^{ext} - C_3 \hat{\tau}_r^{ext}$
$\tau_r = \hat{\tau}_r^{dis} + C_2 q_m - C_r q_r - C_4 \hat{\tau}_m^{ext} - C_6 \hat{\tau}_r^{ext}$
else if $Contact = false$ **then**
$\tau_m = 0$
$\tau_r = \hat{\tau}_r^{dis} + C_2 q_m - C_r q_r$
end if

With this algorithm, when contact is detected four channel teleoperation is implemented between the robots using (12)-(13). In free motion, master robot controller is turned off with $\tau_m = 0$ and C_4, C_6 are set to 0, so that the remote robot only tracks the position of the master.

IV. Experiments

The performance of the proposed X-lateral teleoperation method (PM) was tested on teleoperation systems consisting of 1-DOF linear motors and Phantom Omni robots. For the 1-DOF teleoperation system, 2 brushless linear DC motors (STA1116 by Dunkermotoren) were used. The communication between the computer and motor drivers was realized with two DAQ cards on the same PC (NI-6321e). In Simulink, the *Data Acquisition Toolbox* was used to receive and send signals in real-time. Controller gains for this setup were selected as: $K_p = 700$, $K_d = 3$, $C_f = 1$, $g_{dis} = 500 rad/s$. Phantom Omni robots communicate with the PC through a USB interface and real-time control was realized on Matlab/Simulink using the *PhanTorque* library. In the experiments, the controller gains for Phantom robot joints were selected as $K_p = \{6, 3, 2\}$, $K_d = \{0.08, 0.12, 0.03\}$, $C_f = \{1, 1, 1\}$, $g_{dis} = \{10, 10, 5\} rad/s$. Also, 10 different environments with varying levels of stiffness were used for evaluating system robustness. The experiment setup is shown in Fig. 3-left. 10 different environments including metal, wood, granite, foams, sponges and balloons filled with different amounts of air and water can be seen in Fig. 3-right. Training for contact detection was performed with only the hardest metal surface (a) and softest surface which was a balloon (f). Contact detection performance was evaluated using using linear motors (LM) and Phantom Omnis (PO) on all environments. Overall accuracy and average response

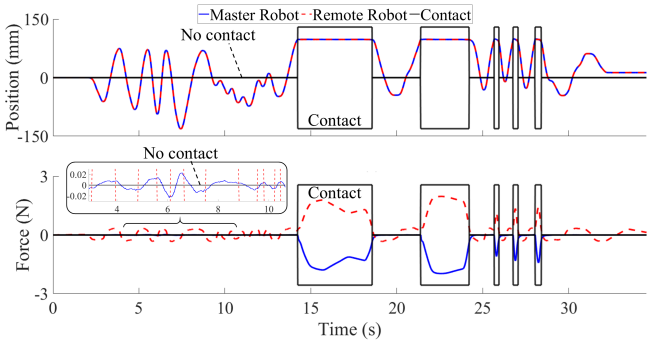

Fig. 4. Position, force responses and the switching signal in Exp. 1.

time in comparison to force sensor data from hundreds of contact/free motion transitions are presented in Table I.

TABLE I

CONTACT DETECTION PERFORMANCE

	Accuracy		Response
	Contact	**Free Motion**	**Time Avg.**
LM	75/81 (93%)	93/95 (98%)	5.80ms
PO	88/100 (88%)	103/106 (97%)	15.00ms

A. Exp 1: Feasibility of X-Lateral Teleoperation

In this experiment, the goal was to evaluate the feasibility of the learning-based contact detection and switching teleoperation method. The experiment setup consisted of two 1-DOF linear motors and wood was selected as the test environment, which was not used in training. The operator moved the master robot back and forth in free motion and after 14 seconds, started contacting the environment repeatedly. Position, force and contact detection algorithm outputs (shown with black boxes when true) are plotted in Fig. 4. Results show that the proposed method could quickly and accurately detect contact, achieve perfect position tracking during both free motion and contact, and force reflection during contact. Furthermore, it can be seen that the operational forces were just the inertial forces and much smaller than the estimated remote robot forces, which would have been reflected to the operator with the conventional approaches.

B. Exp 2: Comparison with Switching Transparency Optimized Two Channel Control [5]

In this experiment, using the 1-DOF teleoperation system we evaluated our controller with 10 different environments shown in Fig. 3 to evaluate the robustness and transparency. We also compared our method with the most similar method in the literature [5] which is a switching two channel

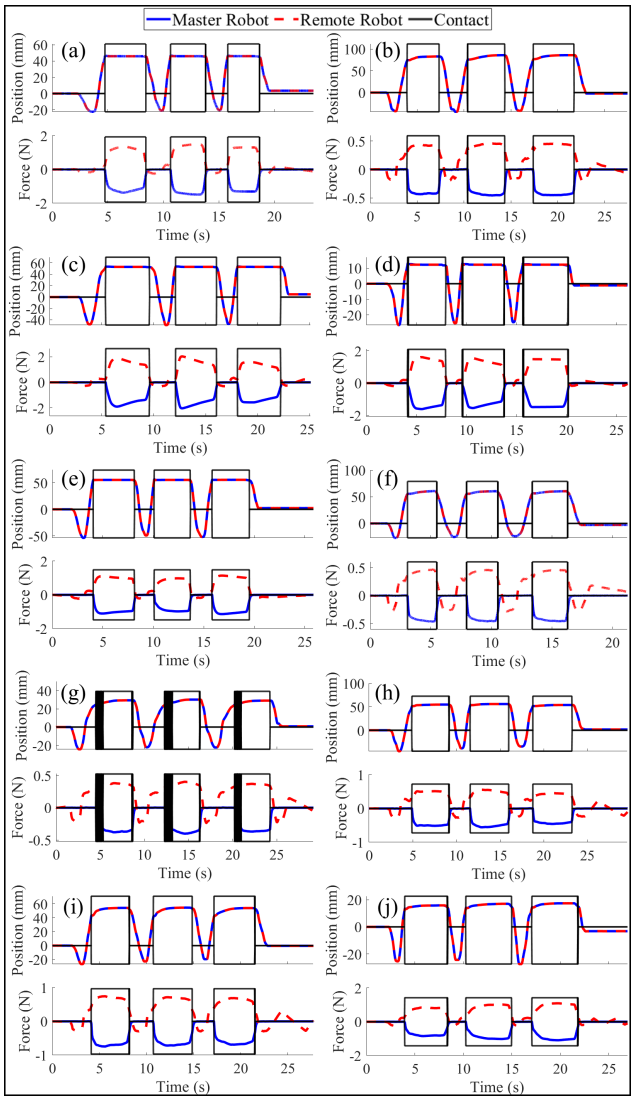

Fig. 5. Position, force responses and switching with proposed method (PM) and environments (a) (b) (c) (d) (e) (f) (g) (h) (i) (j) in Exp 2.

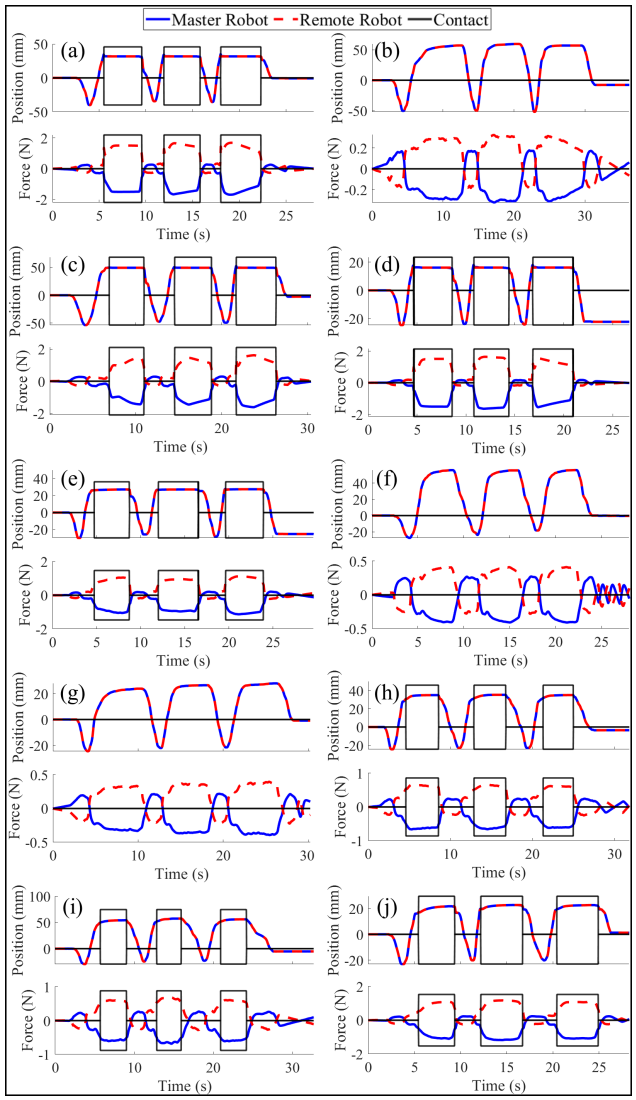

Fig. 6. Position, force responses and switching with the method presented in [5] and environments (a) (b) (c) (d) (e) (f) (g) (h) (i) (j) in Exp 2.

TABLE II

RMS ERROR VALUES (N) IN OPERATIONALITY FOR FIG. 5 AND 6 AND SUCCESS OF CONTACT DETECTION

		a	b	c	d	e	f	g	h	i	j	Mean	STD
RMSE	PM	0.03	0.01	0.02	0.02	0.03	0.05	0.01	0.03	0.08	0.06	0.03	0.02
	[5]	0.18	0.12	0.20	0.13	0.15	0.18	0.15	0.20	0.20	0.22	0.17	0.03
		a	b	c	d	e	f	g	h	i	j	Succ.	Fail
Success	PM	✓	✓	✓	✓	✓	✓	×	✓	✓	✓	9	1
	[5]	✓	×	✓	✓	✓	×	×	✓	✓	✓	7	3

controller optimized to achieve the same performance goals as four channel teleoperation (5)-(6). Instead of using all four channels at the same time, this controller utilizes force control on the master side and position control on the remote side (FP) during free motion and position control on the master side and force control on the remote side (PF) during contact. To determine contact, a force threshold of 0.5N on the remote robot side was used which was selected empirically based on maximum free motion force estimates.

Figures 5 and 6 present the position and force response as well as switching signal plots from the proposed method and the method in [5] respectively. Our method successfully identified contact in 9 out of 10 environments. In the soft balloon (g), due to the similarity between free motion and contact forces, high-frequency switching occurred during initial contact, however, the control system was still stable and transparent. Conversely, the threshold method from [5] completely failed to detect contact on soft surfaces (b), (f), and (g) due to the low contact force. The RMS force error values obtained during free motion, which correspond to operational forces, are presented in Table II. It can be seen that operational forces were reduced by 2 to 15 times with the proposed method. The success of different contact detection methods with different surfaces is also provided in Table II.

C. Exp 3: Force Validation using Phantom Omni Robots

In this experiment, the proposed method was implemented on two Phantom Omni haptic devices and was compared with a sensorless four-channel architecture with and without dynamic compensation. The last three passive joints of the Omnis were fixed and the systems were used as 3-DOF robots. To evaluate force feedback accuracy along the contact Z axis, a single DOF force sensor (Burster 8523-50) was utilized as the ground truth and the environment. In the first test of the experiment, a four-channel teleoperation architecture with disturbance observer-based force estimation was implemented, in the second test the inverse dynamics torques of the robots were identified with neural networks and subtracted from the force estimates as suggested in [30], [31]. In the third test, the proposed method was used. The operator teleoperated the remote robot in free motion and made repeated contact with the sensor. The force estimates from the master robots (blue) and remote robots (red) are provided together with the force sensor readings (black) in Fig. 7. The normalized root mean square errors (NRMSE) [32] are provided in Table III.

It can be seen that with the proposed method the error in

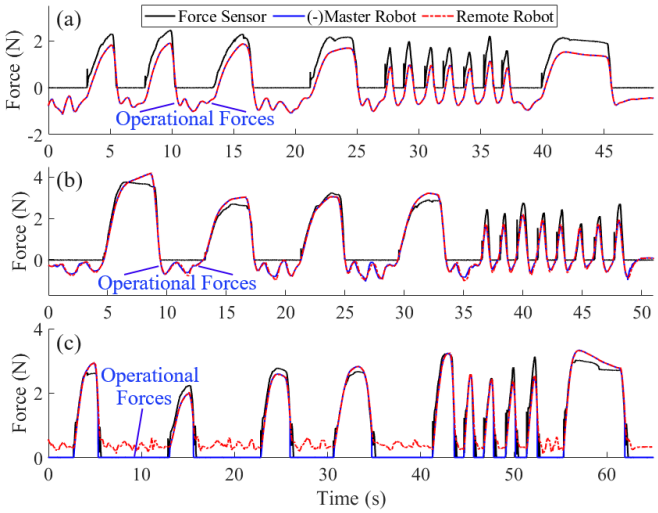

Fig. 7. Teleoperation between 2 Phantom Omni robots (a) Bilateral teleoperation without dynamic compensation and CDA. In FS: 4Ch, In contact: 4Ch (b) Bilateral teleoperation without CDA. In FS: 4Ch, In contact: 4Ch (c) Proposed Method (Switching). In FS: Unilateral, In contact: 4Ch

free motion corresponding to operational force was about 0.28%. This value is roughly 50 times smaller than the dynamic compensated force estimation based four-channel control and almost 100 times smaller than the four-channel controller without dynamic compensation. During contact, the proposed method had less than 10% RMSE, and a comparable performance with dynamic compensation approach. This was significantly better than the approach without compensation at 25% RMSE. Also, the NRMSE value in the entire experiment was about 6% for the proposed method, which was smaller than the other methods.

TABLE III

NORMALIZED RMS ERROR VALUES (%) OF FORCES IN Z-AXIS IN FREE, CONTACT AND ENTIRE MOTIONS FROM EXP. 3 (FIGURE 7)

	Free Motion	Contact Motion	Entire Motion
Test 1 (a)	26.6925	24.6447	25.7614
Test 2 (b)	11.1779	8.8713	10.2259
Test 3 (c)	0.2890	9.5406	6.3726

V. CONCLUSION AND FUTURE WORKS

This paper has proposed a new contact detection based hybrid unilateral/bilateral teleoperation architecture. The proposed method is particularly useful when impedance-type haptic devices with low inertias are used. However, even with admittance-type master manipulators with significant inertia and friction, it should be possible to implement the proposed framework by closing a local force control loop on the master side during unilateral teleoperation to make the system lighter. While experiments have demonstrated significant performance improvements and stable behavior, stability analysis of the proposed hybrid system is a future research goal. Also, while we used multi-class classification here, we aim to compare our method with different classification techniques discussed in the literature.

REFERENCES

[1] B. Hannaford, "A design framework for teleoperators with kinesthetic feedback," *IEEE transactions on Robotics and Automation*, vol. 5, no. 4, pp. 426–434, 1989.

[2] D. A. Lawrence, "Stability and transparency in bilateral teleoperation," *IEEE transactions on robotics and automation*, vol. 9, no. 5, pp. 624–637, 1993.

[3] Y. Yokokohji and T. Yoshikawa, "Bilateral control of master-slave manipulators for ideal kinesthetic coupling-formulation and experiment," *IEEE transactions on robotics and automation*, vol. 10, no. 5, pp. 605–620, 1994.

[4] W. Iida and K. Ohnishi, "Reproducibility and operationality in bilateral teleoperation," in *The 8th IEEE International Workshop on Advanced Motion Control, 2004. AMC'04.* IEEE, 2004, pp. 217–222.

[5] J. Kim, P. H. Chang, and H.-S. Park, "Two-channel transparency-optimized control architectures in bilateral teleoperation with time delay," *IEEE Transactions on Control Systems Technology*, vol. 21, no. 1, pp. 40–51, 2011.

[6] S. Sirouspour and A. Shahdi, "Model predictive control for transparent teleoperation under communication time delay," *IEEE Transactions on Robotics*, vol. 22, no. 6, pp. 1131–1145, 2006.

[7] C. A. L. Martínez, R. van de Molengraft, and M. Steinbuch, "High performance teleoperation using switching robust control," in *2013 World Haptics Conference (WHC)*. IEEE, 2013, pp. 383–388.

[8] C. A. L. Martínez, R. van de Molengraft, S. Weiland, and M. Steinbuch, "Switching robust control for bilateral teleoperation," *IEEE Transactions on Control Systems Technology*, vol. 24, no. 1, pp. 172–188, 2015.

[9] L. Ni and D. W. Wang, "A gain-switching control scheme for position-error-based bilateral teleoperation: Contact stability analysis and controller design," *The International Journal of Robotics Research*, vol. 23, no. 3, pp. 255–274, 2004.

[10] J. An and D.-S. Kwon, "Stability and performance of haptic interfaces with active/passive actuators—theory and experiments," *The International Journal of Robotics Research*, vol. 25, no. 11, pp. 1121–1136, 2006.

[11] M. Lacki and C. Rossa, "Sensorless force approximation control of 3-dof passive haptic devices," in *Smart Multimedia: Third International Conference, ICSM 2022, Marseille, France, August 25–27, 2022, Revised Selected Papers*. Springer, 2022, pp. 381–394.

[12] M. Lkacki and C. Rossa, "Design and control of a 3 degree-of-freedom parallel passive haptic device," *IEEE Transactions on Haptics*, vol. 13, no. 4, pp. 720–732, 2020.

[13] V. J. Lumelsky and E. Cheung, "Real-time collision avoidance in teleoperated whole-sensitive robot arm manipulators," *IEEE Transactions on Systems, Man, and Cybernetics*, vol. 23, no. 1, pp. 194–203, 1993.

[14] M. Strohmayr, "Artificial skin in robotics," 2012.

[15] G. De Maria, C. Natale, and S. Pirozzi, "Force/tactile sensor for robotic applications," *Sensors and Actuators A: Physical*, vol. 175, pp. 60–72, 2012.

[16] R. S. Dahiya, P. Mittendorfer, M. Valle, G. Cheng, and V. J. Lumelsky, "Directions toward effective utilization of tactile skin: A review," *IEEE Sensors Journal*, vol. 13, no. 11, pp. 4121–4138, 2013.

[17] K. Suita, Y. Yamada, N. Tsuchida, K. Imai, H. Ikeda, and N. Sugimoto, "A failure-to-safety" kyozon" system with simple contact detection and stop capabilities for safe human-autonomous robot coexistence," in *Proceedings of 1995 IEEE International Conference on Robotics and Automation*, vol. 3. IEEE, 1995, pp. 3089–3096.

[18] Y. Yamada, Y. Hirasawa, S. Huang, Y. Umetani, and K. Suita, "Human-robot contact in the safeguarding space," *IEEE/ASME transactions on mechatronics*, vol. 2, no. 4, pp. 230–236, 1997.

[19] C.-N. Cho, J.-H. Kim, Y.-L. Kim, J.-B. Song, and J.-H. Kyung, "Collision detection algorithm to distinguish between intended contact and unexpected collision," *Advanced Robotics*, vol. 26, no. 16, pp. 1825–1840, 2012.

[20] S. Takakura, T. Murakami, and K. Ohnishi, "An approach to collision detection and recovery motion in industrial robot," in *15th Annual Conference of IEEE Industrial Electronics Society*. IEEE, 1989, pp. 421–426.

[21] A. De Luca, A. Albu-Schaffer, S. Haddadin, and G. Hirzinger, "Collision detection and safe reaction with the dlr-iii lightweight manipulator arm," in *2006 IEEE/RSJ International Conference on Intelligent Robots and Systems*. IEEE, 2006, pp. 1623–1630.

[22] A. De Luca and R. Mattone, "Actuator failure detection and isolation using generalized momenta," in *2003 IEEE international conference on robotics and automation (cat. No. 03CH37422)*, vol. 1. IEEE, 2003, pp. 634–639.

[23] H. Kuntze, C. W. Frey, K. Giesen, and G. Milighetti, "Fault tolerant supervisory control of human interactive robots," in *IFAC Workshop on Advanced Control and Diagnosis, Duisburg, D*, 2003.

[24] J. Kubık, R. Szadkowski, and J. Faigl, "Learning-based detection of leg-surface contact using position feedback only," *2022 IEEE 27th International Conference on Emerging Technologies and Factory Automation (ETFA)*, 2022.

[25] Y. J. Heo, D. Kim, W. Lee, H. Kim, J. Park, and W. K. Chung, "Collision detection for industrial collaborative robots: A deep learning approach," *IEEE Robotics and Automation Letters*, vol. 4, no. 2, pp. 740–746, 2019.

[26] K. M. Park, J. Kim, J. Park, and F. C. Park, "Learning-based real-time detection of robot collisions without joint torque sensors," *IEEE Robotics and Automation letters*, vol. 6, no. 1, pp. 103–110, 2020.

[27] K. M. Park, Y. Park, S. Yoon, and F. C. Park, "Collision detection for robot manipulators using unsupervised anomaly detection algorithms," *IEEE/ASME Transactions on Mechatronics*, 2021.

[28] K. Narukawa, T. Yoshiike, K. Tanaka, and M. Kuroda, "Real-time collision detection based on one class svm for safe movement of humanoid robot," in *2017 IEEE-RAS 17th International Conference on Humanoid Robotics (Humanoids)*. IEEE, 2017, pp. 791–796.

[29] T. Chen, X. Liu, B. Xia, W. Wang, and Y. Lai, "Unsupervised anomaly detection of industrial robots using sliding-window convolutional variational autoencoder," *IEEE Access*, vol. 8, pp. 47 072–47 081, 2020.

[30] N. Yilmaz, J. Y. Wu, P. Kazanzides, and U. Tumerdem, "Neural network based inverse dynamics identification and external force estimation on the da vinci research kit," in *2020 IEEE International Conference on Robotics and Automation (ICRA)*. IEEE, 2020, pp. 1387–1393.

[31] N. Yilmaz, M. Bazman, and U. Tumerdem, "External force/torque estimation on a dexterous parallel robotic surgical instrument wrist," in *2018 IEEE/RSJ International Conference on Intelligent Robots and Systems (IROS)*. IEEE, 2018, pp. 4396–4403.

[32] F. Piqué, M. N. Boushaki, M. Brancadoro, E. De Momi, and A. Menciassi, "Dynamic modeling of the da vinci research kit arm for the estimation of interaction wrench," in *2019 International Symposium on Medical Robotics (ISMR)*. IEEE, 2019, pp. 1–7.